

Environmentally responsive surface-modified silica nanoparticles for enhanced oil recovery

Abed Behzadi · Aliasghar Mohammadi

Received: 28 February 2016 / Accepted: 24 August 2016 / Published online: 1 September 2016
© Springer Science+Business Media Dordrecht 2016

Abstract Environmentally responsive surface-modified nanoparticles are colloidal nanoparticles coated with, at least, two physicochemically distinct surface groups. Recent advances in the synthesis and production of nanoparticles have enabled the production of environmentally responsive surface-modified nanoparticles with both hydrophilic and hydrophobic surface groups. These nanoparticles act like colloidal surfactants. In this paper, environmentally responsive surface-modified silica nanoparticles are synthesized and used for enhancement of oil recovery. For this purpose, silica nanoparticles are coated with polyethylene glycol chains as hydrophilic agent and propyl chains as hydrophobic agent at various quantities, and their ability to modulate oil–water interface properties and oil recovery is examined. Oil–water interfacial tension and water surface tension are decreased by 50 % in the presence of silica nanoparticles coated with both agents. Measuring oil-drop contact angle on oil-wetted glass slides and carbonate rock sections, after aging in various surface-modified silica nanofluids, indicates that the wettability of various oil-wetted surfaces is modified from strongly oil-wet to water-wet. Flooding nanofluids to glass micro-models and pore-level investigations demonstrate that surface modification of silica nanoparticles, specially, with both hydrophilic and hydrophobic

agents improves considerably their performance in increasing oil recovery and wettability alteration.

Keywords Silica nanoparticle · Surface modification · Nanofluid · Enhanced oil recovery · Energy resources

Introduction

Crude oil is the most widely used source of energy in the world. Major portions of the crude oils are produced from oil reservoirs through conventional oil recovery processes (including the primary and secondary oil recovery processes) (Thomas 2008). On average, only about a third of the oil in place can be recovered by conventional oil recovery processes. Hence, developing more and more efficient techniques to enhance oil recovery, the so-called enhanced oil recovery (EOR), is inevitable (Green and Willhite 1998). EOR processes include thermal (Clark et al. 2010; Kamal et al. 2014), chemical (Watkins 2009), and microbial (Dietrich et al. 1996; Sen 2008), which are based on interfacial tension reduction (Barnes et al. 2012; Green and Willhite 1998; Hirasaki et al. 2008), viscosity control (Bauer and Klemmensen 1982; Jamaloei and Kharrat 2010; Ramirez 1987), and wettability alteration (Morrow 1990; Somasundaran and Zhang 2006; Zhao et al. 2010).

Among the EOR processes, chemical-assisted enhanced oil recovery processes (CEOR) have

A. Behzadi · A. Mohammadi (✉)
Department of Chemical and Petroleum Engineering,
Sharif University of Technology, Tehran, Iran
e-mail: amohammadi@sharif.edu

increasingly come into focus due to the provided ability of controlling the properties of crude oil–formation water and reservoir rock–crude oil–formation water interfaces using chemical agents (Mohammed and Babadagli 2015). Chemicals used in CEOR are mostly polymers (Kang et al. 2011; Shaker Shiran and Skauge 2013) and surfactants (Johannessen and Spildo 2013; Puerto et al. 2012). Polymers improve oil recovery by increasing the viscosity of injecting fluid and controlling the oil and injecting fluid mobility, while surfactants perform by reducing interfacial tension (Bera et al. 2013; Rosen et al. 2005) and altering reservoir rock wettability (Al-Sulaimani et al. 2012; Chaudhuri and Paria 2014). Polymers are potential to chemical or thermal degradation (Levitt and Pope 2008), and their molecular weight is so huge that makes their transport in low permeable media difficult. Flooding surfactants have limited performance in CEOR when salinity and temperature are high, and most of surfactants are prone to hydrolysis. These problems resulted in investigations for new and efficient materials for CEOR. Thus, of other chemicals that have found various applications in CEOR are nanoparticles that their application in CEOR is interested mainly due to their ability to modulate interfacial tension and alternate reservoir rock wettability.

There have been extensive studies on whether and how nanoparticles alter wettability of oil-wet or medium-wet surfaces to more water-wet states. In an experimental attempt by Suleimanov et al. (2011), the impact of a nonferrous metal nanoparticle on the wettability alteration property of anionic surfactants was studied by measurements of contact angles, observing that contact angles are not changed and indicating that wettability is not modulated by the metal nanoparticle. They concluded that the enhancement of oil recovery in the presence of nanoparticles is due to the decrease in the interfacial tension and the change in the flow characteristics of injecting fluid. Karimi et al. (2012) studied the wettability alteration with a nanofluid containing zirconium dioxide nanoparticles and nonionic surfactants in a carbonate reservoir rock. They found a considerable change in the wettability of the rock from the oil-wet to water-wet state. They suggested that the adsorption of the nanoparticles results in the nanoparticle structuring on the rock, and they concluded that the wettability alteration is mainly due to the formation of the

structured nanoparticle layer. Zhang et al. (2014) conducted imbibition tests using a reservoir crude oil and a Berea sandstone treated with a nanofluid containing silica nanoparticles. They showed that the nanofluid is suitable for displacing crude oil from Berea sandstone, especially in a high-salinity environment containing calcium and magnesium ions.

Roustaei and Bagherzadeh (2015) experimentally studied the impact of silica nanoparticles on the wettability of a carbonate reservoir rock. They concluded that a considerable amount of oil can be recovered right after injecting water to the aged core plug with a nanofluid containing silica nanoparticles. More recently, Lim et al. (2015) reported the changes in the wettability of three different solid substrates using a nanofluid composed of silica nanoparticles dispersed in water. They observed that the extent of the wettability alteration depends on the volume fraction of the nanoparticles, their size, and the type of substrate. In addition, they found a strong correlation between the change in the substrate wettability and the nanoparticle volume fraction close to the substrate surface.

Of other experimental attempts, we can mention to the experimental study of Maghzi et al. (2012). They used glass micro-models to examine the effect of silica nanoparticles on the wettability alteration. They found, in waterflooding experiments, that the presence of silica nanoparticles results in a significant enhancement of oil recovery, highlighting the ability of silica nanoparticles to alter glass surface wettability (Maghzi et al. 2012). Also, it is reported that adding silicon dioxide and zirconium dioxide nanoparticles to surfactants solution improves their wettability alteration ability helping EOR processes (Karimi et al. 2012; Le et al. 2011; Zargartalebi et al. 2014).

The aforementioned cases are examples of experimental studies on the wettability alteration properties of nanoparticles among many other experimental reports (see Lim et al. (2015), and references therein). On the other hand, although it is well known that nanoparticles can alter reservoir rock wettability, no consensus has been reached on whether nanoparticles affect oil–water interfacial tension (see Fan and Striolo (2012), and references therein). It is sometimes observed that nanoparticles decrease the interfacial tension, but in some other instances they are observed not to modulate considerably the tension. When significant interfacial tension reduction in the presence

of nanoparticles is observed, it is generally explained by the adsorption of nanoparticles to interfaces.

However, in terms of interfacial tension and reservoir rock wettability alteration, applications of nanofluids for EOR processes arise from their ability to adsorb to interfaces (Binks and Whitby 2004; Wang et al. 2011). The degree of adsorption of nanoparticles onto reservoir rocks' surfaces and at the oil–water interfaces determines the wettability alteration ability and the decrease in interfacial tension. Thus, engineering nanoparticles to adsorb preferentially to interfaces can improve nanofluid surface activity, where this can be achieved through surface modification of nanoparticles.

Surface modification of nanoparticles by covalently attaching polymers to the nanoparticle surface in order to render polymer-coated nanoparticles has received much interest for EOR applications. While less work has been carried out with polymer-coated nanoparticles for EOR processes, emerging literature suggests that they may perform much better than bare (unmodified) nanoparticles for EOR (ShamsiJazeyi et al. 2014). Among all types of polymer-coated nanoparticles, mixed polymer-coated nanoparticles, in which two distinct polymers are randomly coated on the surface of bare nanoparticles, are particularly interesting as they can be designed to exhibit responsive properties under environmental variations (Zhao and Zhu 2009). The coexistence of, at least, two kinds of polymers on the nanoparticle surface may endow the nanoparticles responsiveness, for example, to solvent, temperature, pH, and light, by controlling proper chemical composition.

Recent advances in the synthesis and production of surface-modified nanoparticles have enabled the production of environmentally responsive mixed polymer-coated nanoparticles with both hydrophilic and hydrophobic surface groups. These nanoparticles in a suspension act like surfactant molecules (see Zhao and Zhu (2009), and references therein). For example, like surfactant molecules can attach to fluid–fluid interfaces to form a monolayer. In addition, they, like surfactant molecules, are used to stabilize multiphase systems. For instance, there have been experimental efforts on the application of surface-modified silica nanoparticles with a constant modifying agent quantity for stabilizing oil–water emulsions (Wang et al. 2010), as well as investigating nanoparticle dispersion rheology and adsorption behavior on reservoir rocks

surfaces (Rodriguez Pin et al. 2009). In summary, environmentally responsive mixed polymer-coated nanoparticles may exhibit synergistic abilities of both surfactants and nanoparticles.

In spite of extensive studies on the performance of unmodified nanoparticles and surfactant molecules for enhanced oil recovery, less work has been reported on the performance of environmentally responsive mixed polymer-coated nanoparticles for oil recovery-oriented applications. Of the few studies, we can mention to the EOR-oriented application of surface-modified nanoparticles with both hydrophilic and hydrophobic polymers in order to control the stability of foams used to recover hydrocarbons from underground formations (Baran and Cabrera 2006). The use of surface-modified nanoparticles resulted in foams that were stable under pressure yet had a shorter foam lifetime than typical surfactant-stabilized foams after the pressure was lowered.

A thorough understanding of the environmentally responsive mixed polymer-coated nanoparticles' behavior in contact with reservoir fluids and the walls of rock's pores can help to improve enhanced oil recovery processes. This can be achieved through systematic studies to develop a more comprehensive understanding of how environmentally responsive mixed polymer-coated nanoparticles alter the properties of oil–water and oil–water–solid interfaces. For this purpose, we are aimed, in this paper, to investigate the impact of silica nanoparticles surface modification on their performance in increasing oil recovery and wettability alteration. Silica nanoparticles are interested for EOR-oriented applications due to their low cost and availability. Also, modifying silica nanoparticles is experimentally possible due to silanol groups on their surface. These groups can react with organofunctional alkoxysilanes to create a chemical bond between silica nanoparticle surface and organofunctional groups.

In this study, polyethylene glycol chains as hydrophilic agent and propyl chains as hydrophobic agent are randomly coated on silica nanoparticle surface. Surface modification of silica nanoparticles by both agents is carried out to create environmentally responsive nanoparticles with different ratios of modifying agents' quantity to silica nanoparticle's quantity. Fourier transform infrared (FT-IR) spectroscopy is used to examine nanoparticles surface modification. The surface activity of nanofluids

containing the nanoparticles is studied by measuring oil–water interfacial tension and water surface tension in the presence of silica nanoparticles. Also, the wettability alteration is investigated by measuring oil-drop contact angle on two different oil-wetted surfaces after aging in nanofluids containing the nanoparticles. Then, the surface-modified nanoparticles performance in EOR processes is examined via monitoring wettability alteration and oil recovery factor during flooding to a glass micro-model.

Experiments and procedures

In this section, we discuss the materials and method used for fabricating surface-modified nanoparticles and the procedures employed to characterize the nanoparticles and perform oil recovery experiments.

Materials

Our experiments were performed using silica nanoparticles, modifying agents and a sample of crude oil. Non-functionalized, non-porous silica nanoparticles (AEROSIL® 200) provided by the manufacturer as a powder with specific area and average primary diameter $200 \pm 25 \text{ m}^2/\text{g}$ and 12 nm, respectively (as specified by the manufacturer). Also from the manufacturer's reports, SiO_2 content of the nanoparticles is 99.8 wt%, and pH of 4 wt% nanoparticles dispersion in water is in the range of 3.7–4.8. The crude oil was a dead oil from Ahvaz (south of Iran) reservoirs with 5 wt% asphaltene components, 6 wt% resin components, and 14 wt% aromatic components. For all the experiments, freshly prepared double-distilled water, with the conductivity of $1.5 \mu\text{S}/\text{cm}$ measured at $22 \text{ }^\circ\text{C}$, was used. Carbonate rock sample was from Ali-goodarz mine located in southwest of Iran. Rock sample purity was $\sim 99 \%$ (based on reported analysis by Zagros powder company) (Monfared et al. 2015). XRD spectrum from the rock sample is shown in Fig. 1. Hydrophilic agent was polyethylene glycol linked to 3-glycidoxypropyltrimethoxysilane (3-GTO/MPEG), which was synthesized from polyethyleneglycholmethylether (MPEG, average $M_n \sim 2000$, Sigma-Aldrich) and 3-glycidoxypropyltrimethoxysilane (3-GTO, Sigma-Aldrich, 98 %). Hydrophobic agent coated on silica nanoparticle was trimethoxy(propyl)silane (C3S, Sigma-Aldrich,

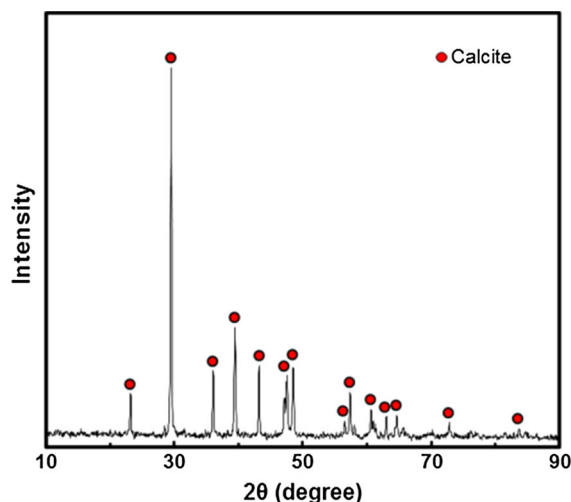


Fig. 1 XRD pattern of carbonate rock sample (Monfared et al. 2015)

97 %). Other chemicals used were acetic acid (Merck, glacial, 100.0 %), ammonia (Merck, solution of 29.3 %, extra pure), acetonitrile (Ameretat Shimi, 99.9 %), ethanol (Hamon teb markazi, 96.2 vol.%), and toluene (Ameretat Shimi, 99.9 %).

Nanoparticles surface modification

In general, the surface modification of silica nanoparticles is achieved through functionalizing silanol groups, which exist on the surface of silica nanoparticles, with suitable silane reagents. Of our two agents, i.e., MPEG and C3S, which are to be covalently attached to the silica nanoparticle surface, only C3S has suitable silane groups. Accordingly, in order to covalently attach MPEG to the silica nanoparticle surface, MPEG must be functionalized with a suitable silane reagent. To this end, 3-GTO, which contains suitable silane groups, was chemically linked to MPEG; this procedure yielded hydrophilic agent, i.e., 3-GTO/MPEG.

For the purpose of chemically linking 3-GTO to MPEG, at the beginning, MPEG, in order to be dried from any traces of water, was melted by heating at $80 \text{ }^\circ\text{C}$ for 3 h. Then, 30 g of the dried MPEG was poured into 150 mL of acetonitrile, and 3.9 g of 3-GTO was added to the solution. Subsequently, 0.2 mL of acetic acid as catalyzer was mixed with the solution. The resulting solution was refluxed at $90 \text{ }^\circ\text{C}$ with continuous stirring for 6 h. The solvent was

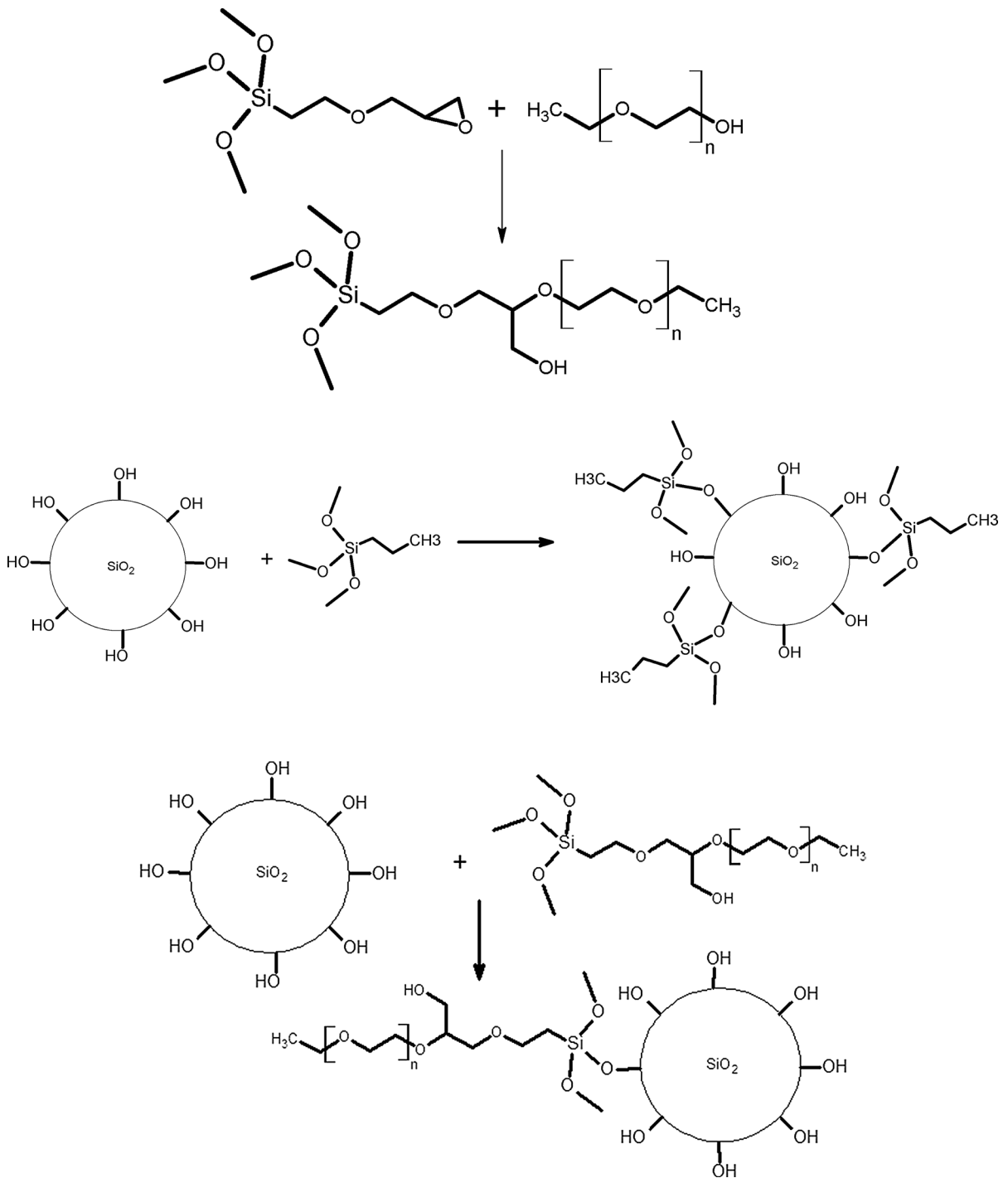


Fig. 2 Chemical reaction steps used for (*upper panel*) 3-GTO/MPEG synthesis from 3-GTO and MPEG, (*middle panel*) hydrophobic silica nanoparticle synthesis from C3S and silica

nanoparticle, and (*lower panel*) hydrophilic silica nanoparticle synthesis from 3-GTO/MPEG and silica nanoparticle

Table 1 Quantity of modifying agents used for coating silica nanoparticles

Nanofluid no.	Q_{HPI}	Q_{HPO}
1	0	1.22×10^{-3}
2	0	0.75×10^{-3}
3	5.71×10^{-3}	0
4	3.22×10^{-3}	0
5	5.71×10^{-3}	0.37×10^{-3}
6	1.72×10^{-3}	0.75×10^{-3}
7	3.22×10^{-3}	0.56×10^{-3}

Q_{HPI} hydrophilic modifying agent quantity in mol/(g nanoparticle)

Q_{HPO} hydrophobic modifying agent quantity in mol/(g nanoparticle)

removed from products by evaporation. Chemical reaction step used for chemically linking 3-GTO to MPEG is shown in the upper panel of Fig. 2.

Then, we coated 3-GTO/MPEG and C3S on the silica nanoparticle surface. For this purpose, the alkoxy silane groups of 3-GTO/MPEG and C3S should be hydrolyzed to produce silanol groups. Thus, 3-GTO/MPEG and C3S were hydrolyzed by adding 30 mol equivalent of water (with pH 9.5 set by 0.1 M NaOH solution) with continuous stirring for 3 h. Subsequently, hydrolyzed agents were injected dropwise (in 1 h using a syringe pump) into 5 wt% silica nanofluid (which was prepared through dispersing 2 g of silica nanoparticles in 38 g of double-distilled water by probe sonication for 6 min) with pH 9.5 set by 0.1 M NaOH solution. The reaction mixture was then refluxed at 80 °C under continuous stirring. Total reaction time was 12 and 5 h for coating 3-GTO/MPEG and C3S, respectively. Chemical reaction steps used for coating C3S and 3-GTO/MPEG on silica surface are shown in the middle and lower panels of Fig. 2, respectively. Coating both agents on silica nanoparticles surface was performed by initially coating C3S, and then, by grafting 3-GTO/MPEG.

After coating agents on silica nanoparticles, nanoparticles were collected from unreacted agents and suspending medium (which was water) and washed with double-distilled water and ethanol by four times centrifugation, at 10,000 rpm for 6 min, and decantation (three times with double-distilled water, and then, once with ethanol). Then, the collected nanoparticles were dried by heating at 70 °C for 12 h in an oven, and subsequently, the

dried nanoparticles were suspended in double-distilled water to have aqueous stock solutions at a concentration 10 wt%. Table 1 presents the quantities of modifying agents used for coating silica nanoparticles surface on the basis of reaction efficiency investigated in Klint (2011) for seven silica nanoparticle samples studied here.

Characterization tests

Dynamic light scattering (DLS), conducted with a Nano S instrument (Malvern Instruments) at 20 °C, was used to determine the hydrodynamic size distribution of silica nanoparticles dispersed in double-distilled water at various nanoparticle concentrations of 0.005, 0.05, 0.5, and 5 wt%. DLS measures the intensity of the laser light scattered from suspending nanoparticles, where the hydrodynamic diameter is obtained from the temporal evolution of the scattered light intensity using the well-known Stokes–Einstein relation (Jiang et al. 2009; Suttiponparnit et al. 2011).

There are a number of techniques to characterize nanoparticles at each stage of surface modification including thermo-gravimetric analysis (TGA), differential scanning calorimetry (DSC), scanning electron microscopy (SEM), and FT-IR spectroscopy. We used FT-IR spectroscopy to monitor desired reactions in surface modification steps. For this purpose, FT-IR spectra were recorded using a 155S MB-series instrument (ABB Bomem) from unmodified silica nanoparticles, 3-GTO, C3S, and MPEG as reactants and from 3-GTO/MPEG, hydrophobic silica nanoparticles, and hydrophilic silica nanoparticles as products. The spectra were measured for modified silica nanoparticles after filtration and drying at 60 °C.

Surface and interfacial tensions and contact angle measurements

We measured oil–water interfacial tension and water surface tension in the presence of our unmodified and surface-modified silica nanoparticles to monitor the surface activity properties of the nanoparticles. For this purpose, surface and interfacial tensions were determined by pendant drop method. Laboratory temperature was ~29 °C when surface and interfacial tension measurements were taken. Reported surface and interfacial tensions are average of those of three different measurements in each sample.

Wettability alteration properties of our unmodified and surface-modified silica nanoparticles were monitored by measuring droplet contact angles of oil–water on oil-wetted solid surfaces using captive drop technique. Solid surfaces were carbonate rock sections and glass slides, where carbonate rock sections were aged in the crude oil for 4 months and glass slides were put in a solution of C3S and toluene at a concentration 1 vol.% for 24 h to alternate their wettability to oil-wet. In captive drop technique, an oil droplet was released and captured below the glass slide or rock section, which was submerged in water. Side images of oil droplets captured below the slide or section were taken and analyzed, and the contact angles were measured through the denser phase (water or silica nanofluids). Accordingly, the contact angles of 0° and 180° correspond, respectively, to a surface completely water- or oil-wet.

To examine the effect of nanoparticles surface modifications on the wettability alteration ability, oil-wetted glass slides and sections were aged in various 1 wt% surface-modified silica nanofluids. Then, captive droplet contact angles of oil–water on the glass slides and sections were measured after 24 and 72 h.

Flooding to glass micro-model

Micro-models are used to replicate porous media in order to visualize transport processes at the pore scale. Most micro-models contain etched or lasered porous substrates or simple pore networks. Micro-models are made from transparent material so that they can be viewed with a microscope; this feature allows fluid flow analysis at the pore-level. In this paper, we performed flooding experiments using a five-spot micro-model system. The glass micro-model was fabricated from two glass slides with the thicknesses of 2 and 4 mm. The desired pattern of porous media, depicted in Fig. 3, was lasered on the 4-mm-thick glass slide. The glasses were bonded at 670°C for 2 h and then cooled to ambient temperature in 24 h. The micro-model wettability was altered from hydrophilic to hydrophobic by injecting a solution of ethanol, double-distilled water, C3S, and ammonia into the model. After reaction at room temperature for 24 h, the solution was withdrawn and the micro-model was rinsed with double-distilled water.

Two series of flooding experiments were conducted. One was with the water-wet micro-model

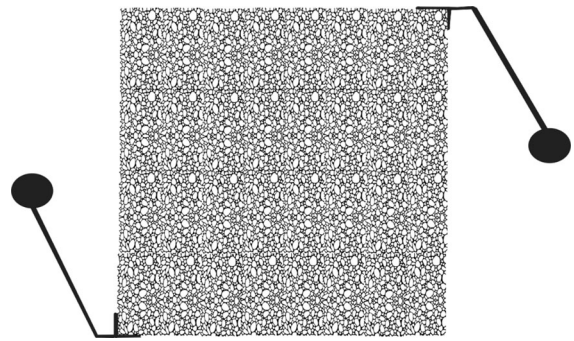


Fig. 3 Pattern lasered on glass as porous media

(before wettability alteration), and the other one was with the oil-wet micro-model (after wettability alteration). In the former case, the water-wet micro-model was initially loaded by the crude oil. By processing the image of the oil-loaded micro-model, the micro-model porosity was determined. Then, double-distilled water was injected into the micro-model by a syringe pump at the rate of 0.1 mL/h. By analyzing the images captured from the micro-model during the flooding of water, recovery factor versus injected pore volume was monitored.

In the latter case, the oil-wet micro-model was initially loaded by the crude oil. Then, unmodified silica nanofluid and nanofluids no. 1, 3, 5, and 6 were injected at the nanoparticle concentration of 1 wt% into the micro-model at the rate of 0.1 mL/h. By processing images of the micro-model when nanofluids were flooding, recovery factor versus injected pore volume was determined. After each flooding test, the micro-model was rinsed with double-distilled water, toluene, and ethanol and then dried at 150°C for 20 min to be refreshed for new flooding test. Also, microscale images were captured from micro-model pores and throats when flooding experiments were being conducted.

Results and discussion

In what follows, the results are reported and discussed. At the beginning, the results of our characterization tests including DLS and FT-IR are examined (“[Dynamic light scattering](#)” and “[Fourier transform infrared spectroscopy](#)” sections). Then, the modulation of oil–water interfacial tension and water surface tension in the presence of our unmodified and surface-

modified silica nanoparticles are presented (“[Surface and interfacial tensions](#)” and “[Contact angle](#)” sections), and it is observed that the surface modification of silica nanoparticles considerably alters the tensions. Afterward, we report the wettability alteration of oil-wetted glass and carbonate rock surfaces in the presence of the unmodified and surface-modified silica nanoparticles, and it is demonstrated that the surface modification of silica nanoparticles significantly alters the wettability of solid surfaces. Finally, oil recoveries obtained by flooding our various unmodified and surface-modified nanofluids to a five-spot glass micro-model are presented (“[Flooding to glass micro-model](#)” section), highlighting the significant improvement in oil recovery by flooding nanofluids containing surface-modified silica nanofluids.

Dynamic light scattering

The unique features that make nanoparticles desirable for EOR-oriented applications are a direct consequence of increased surface-to-volume ratio and their small size (Kim et al. 2016). The agglomeration results in a decrease in the surface-to-volume ratio, and also, fewer available surface groups compared to individual nanoparticles (Hotze et al. 2010; Jassby 2011; Jiang et al. 2009). Thus, the agglomeration of nanoparticles must modulate their ability in EOR processes. The surface activity of nanoparticles depends greatly on their available surface groups, and the agglomeration diminishes their ability in wettability alteration and interfacial tension reduction. Furthermore, the agglomeration results in increased size, leading to adverse effects on porosity and permeability of porous media and reduction in oil recovery (Mohammed and Babadagli 2015). Accordingly, characterizing the agglomeration state of nanoparticles is imperative for EOR-oriented applications.

The primary method for monitoring the agglomeration of nanoparticles is through measuring particle size at various concentrations. In this vein, the hydrodynamic size distribution of our unmodified silica nanofluid at various concentrations measured by DLS is shown in Fig. 4. At the lowest silica nanoparticle concentration (0.005 wt%), the size distribution is reasonably symmetric with a peak at around 200 nm, which is well above the primary nanoparticle size. At the higher nanoparticle concentration

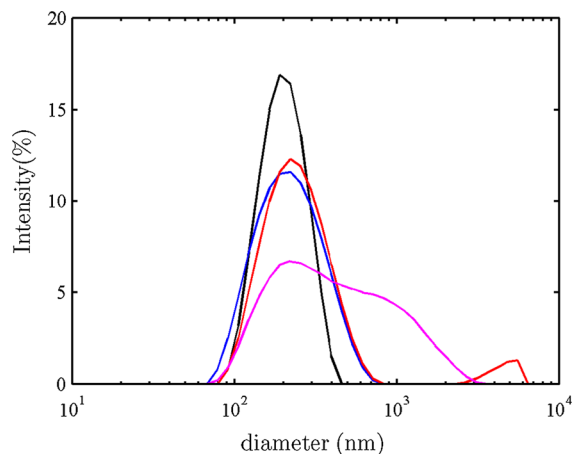


Fig. 4 DLS measurements of the hydrodynamic size distribution of unmodified silica nanofluid at various concentrations of 0.005 (black line), 0.05 (blue line), 0.5 (red line), and 5 (magenta line) wt%. Solvent was double-distilled water. (Color figure online)

(0.05 wt%), the measured size distribution shows slight growth in the nanoparticle hydrodynamic size, and the hydrodynamic size distribution becomes asymmetric, which suggests increased agglomeration of the nanoparticles in the nanofluid. Evidently, at the highest nanoparticle concentration examined (5 wt%), two relatively overlapped wide peaks are observed at around 200 and 1000 nm, which indicates that significant agglomeration takes place, and large flocs are observed.

The hydrodynamic size distributions, depicted in Fig. 4, demonstrate that the agglomeration of our unmodified silica nanoparticles increases with increasing the nanoparticle concentration. The agglomeration of nanoparticles is controlled by nanoparticle–nanoparticle interaction. A classical theory for determining the interaction is based on the Derjaguin–Landau–Verwey–Overbeek (DLVO) theory, which states that the interaction is the sum of the repulsive electrostatic and attractive van der Waals interactions (see Metin et al. (2012), and references therein). Ostensibly, in our unmodified silica nanoparticle dispersions, the electrostatic repulsive interaction is not dominant to prevent the agglomeration, and the increased concentration results in enhanced coagulation rates and larger hydrodynamic sizes. However, the hydrodynamic size is well below glass micro-model pore size, and it does not make any nanoparticles congestion when flooding experiments are being conducted.

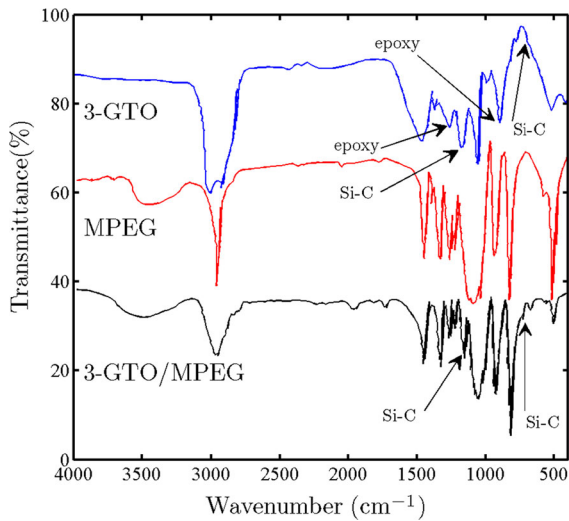


Fig. 5 FT-IR spectra of 3-GTO, MPEG, and 3-GTO/MPEG

Fourier transform infrared spectroscopy

FT-IR spectra of 3-GTO and MPEG as reactants of hydrophilic modifying agent synthesis and 3-GTO/MPEG as product are depicted in Fig. 5. 3-GTO FT-IR spectrum consists of absorption peaks for $-\text{CH}_2$ and $-\text{CH}_3$ groups at $2800\text{--}3000$ and $1250\text{--}1500$ cm^{-1} (Coates 2000). The peak at ~ 1100 cm^{-1} , assigned to Si-O-C and C-O-C groups (Coates 2000) (one is behind the other), is also observed in 3-GTO/MPEG FT-IR spectrum. Absorption peaks attributed to 3-GTO epoxy ring at 1250 and 890 cm^{-1} (Coates 2000) do not appear in 3-GTO/MPEG spectrum. MPEG FT-IR spectrum consists of absorption peaks for $-\text{CH}_2$ and $-\text{CH}_3$ groups at $2800\text{--}3000$ and $1250\text{--}1500$ cm^{-1} (Coates 2000). The peak at 3500 cm^{-1} in MPEG FT-IR spectrum is from $-\text{OH}$ group (Coates 2000), which is also appeared in 3-GTO/MPEG FT-IR spectrum. Also, MPEG spectrum consists of the absorption peak at ~ 1100 cm^{-1} assigned to C-O-C groups. The peak is observed in 3-GTO/MPEG FT-IR spectrum, too. Disappearance of the epoxy ring peak and the appearance of Si-C and Si-O-C groups peaks in 3-GTO/MPEG FT-IR spectrum demonstrate that the desired reaction, shown in the upper panel of Fig. 2, had been carried out.

FT-IR spectra of C3S, unmodified silica nanoparticle, and hydrophobic silica nanoparticle are depicted in Fig. 6 (upper panel). C3S FT-IR spectrum represents absorption peaks at $2800\text{--}3000$ and

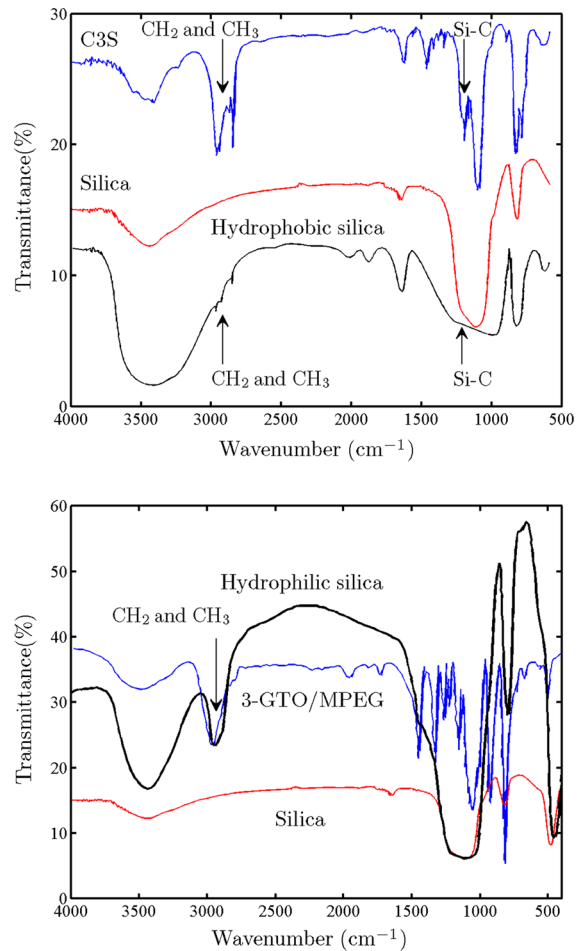


Fig. 6 (Upper panel) FT-IR spectra of C3S, silica nanoparticle, and hydrophobic silica nanoparticle; (lower panel) FT-IR spectra of 3-GTO/MPEG, silica nanoparticle, and hydrophilic silica nanoparticle

$1250\text{--}1500$ cm^{-1} assigned to $-\text{CH}_2$ and $-\text{CH}_3$ groups (Rostami et al. 2011). Absorption peaks of $-\text{CH}_2$ and $-\text{CH}_3$ groups at $2800\text{--}3000$ cm^{-1} are also observed in the modified silica nanoparticle spectrum. Moreover, C3S and silica nanoparticle FT-IR spectra reveal peaks at 800 , 1640 , 1100 , 1200 , and 3400 cm^{-1} assigned to Si-OH, Si-O-C, Si-C, and water (Rostami et al. 2011). Si-C absorption peaks at ~ 700 and 1200 cm^{-1} (Rostami et al. 2011) are also observed in hydrophobic silica nanoparticle FT-IR spectrum (at 1200 cm^{-1} appears like a shoulder). Accordingly, it may be concluded that the cross-linking reaction of C3S and silica nanoparticle, shown in the middle panel of Fig. 2, had been carried out.

Table 2 Surface and interfacial tensions of unmodified silica nanofluids at various silica nanoparticle concentrations

Concentration (wt%)	Surface tension (mN/m)	Interfacial tension (mN/m)
Pure water	71.4 ± .2	28.2 ± .4
0.01	71.5 ± .2	28.3 ± .2
0.1	69.5 ± .2	28.1 ± .3
1	68.1 ± .4	27.3 ± .6
5	66.2 ± .3	
10	65.8 ± .3	

FT-IR spectra of 3-GTO/MPEG and silica nanoparticle as reactants and hydrophilic silica nanoparticle as product are shown in Fig. 6 (lower panel). These spectra indicate that -CH₂ and -CH₃ absorption peaks of 3-GTO/MPEG also appear in the product. Furthermore, C-O-C group absorption peak of 3-GTO/MPEG is observed in the resulting silica nanoparticle FT-IR spectrum. These findings indicate that 3-GTO/MPEG was bonded to silica surface.

Surface and interfacial tensions

Measured surface and interfacial tensions of our unmodified silica nanofluids at various concentrations of nanoparticles are presented in Table 2, and Figs. 7 and 8 (upper panels, green dashed lines). Evidently, the tensions are slightly reduced in the presence of the nanoparticles. This observation arises from the hydrophilic nature of unmodified silica nanoparticles, due to silica -Si-OH surface groups, where the nanoparticles tend to stay away from air-water and oil-water interfaces. In other words, our unmodified silica nanoparticles do not adsorb considerably at the air-water and oil-water interfaces.

In order to have a quantitative measure of how many nanoparticles adsorb at the air-water or oil-water interfaces, we can use the Gibbs adsorption isotherm, which relates the changes in the concentration of a species adsorbed at an interface to the changes in the surface or interfacial tension (Hunter 2001)

$$\Gamma_2 = -\frac{1}{RT} \left(\frac{\partial \gamma}{\partial \ln C_2} \right)_{T,P}, \tag{1}$$

where Γ_2 is the surface concentration of the species at the interface, R the universal gas constant, T the absolute temperature, C_2 the bulk concentration of the species, and γ the surface or interfacial tension.

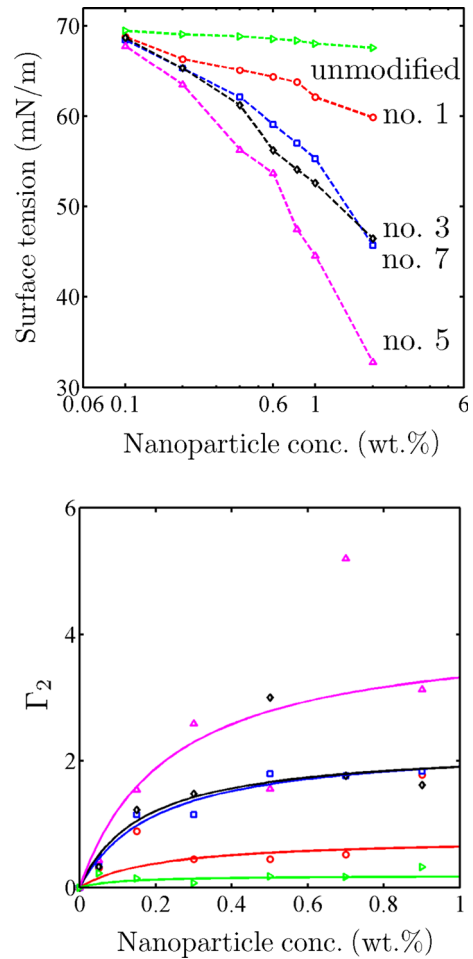


Fig. 7 (Upper panel) Surface tensions of various silica nanofluids versus silica nanoparticle concentration; (lower panel) the surface concentration of the silica nanoparticles adsorbed at air-water interface, calculated using Eq. (1), versus silica nanoparticle concentration. The nanofluids are unmodified (green symbols and lines), no. 1 (red symbols and lines), 3 (black symbols and lines), 5 (magenta symbols and lines), and 7 (blue symbols and lines). Solid lines in the lower panel are the Langmuir adsorption isotherm, Eq. (2), fitted to the data. (Color figure online)

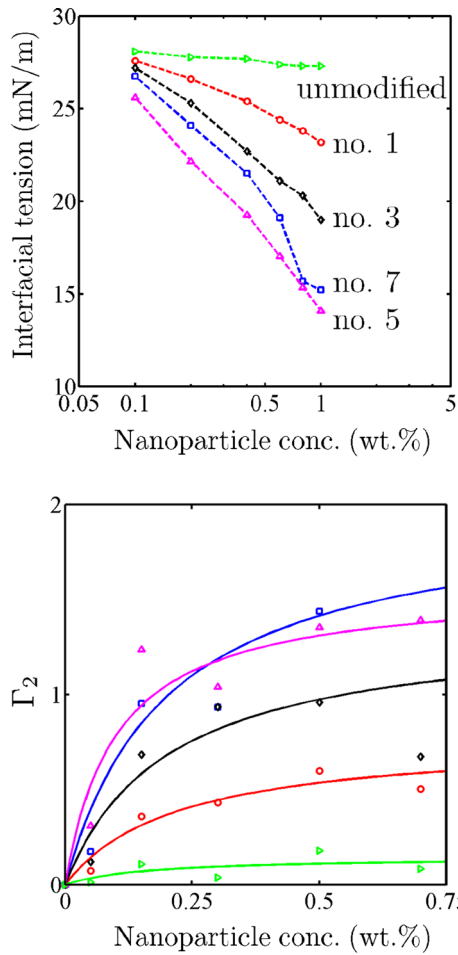


Fig. 8 (Upper panel) Interfacial tensions of various silica nanofluids versus silica nanoparticle concentration; (lower panel) the surface concentration of the silica nanoparticles adsorbed at oil–water interface, calculated using Eq. (1), versus silica nanoparticle concentration. The nanofluids are unmodified (green symbols and lines), no. 1 (red symbols and lines), 3 (black symbols and lines), 5 (magenta symbols and lines), and 7 (blue symbols and lines). Solid lines in the lower panel are the Langmuir adsorption isotherm, Eq. (2), fitted to the data. (Color figure online)

Using Eq. (1), the surface concentration of our unmodified silica nanoparticles at the air–water and oil–water interfaces was obtained, and the results are presented in Figs. 7 and 8 (lower panels, green symbols). Also shown in Figs. 7 and 8 (lower panels, green solid lines) is the fitted model corresponding to the Langmuir adsorption isotherm, which is

$$\Gamma_2 = \Gamma_{\max} \frac{bC_2}{1 + bC_2}, \tag{2}$$

where Γ_{\max} is the maximum surface concentration of the species at the interface. The fitted model, Eq. (2), yields the maximum unmodified silica nanoparticle surface concentrations of $\Gamma_{\max} = 0.19$ and 0.15 nanoparticles/nm² at air–water and oil–water interfaces, respectively.

Now let us focus on the impact of the surface modification of nanoparticles on the surface activity of nanofluids, which was examined by measuring the surface and interfacial tensions of surface-modified silica nanofluids. Results for the surface tensions of surface-modified silica nanofluids are presented in Table 3 and Fig. 7 (upper panel). With increasing each modifying agent quantity on silica surface, the surface tension is modulated much more. Also, it is observed that coating PEG on silica surface modulates the surface tension much more than coating propyl group. This results from the smaller chain of propyl group compared with that of PEG group. In other words, the propyl does not give enough hydrophobicity to silica surface in order to migrate the modified nanoparticle to the air–water interface. In order to give more hydrophobicity to silica surface, larger hydrocarbon chains may be coated on the nanoparticles, where this will be addressed in future works.

The surface concentrations of our surface-modified silica nanoparticles at the air–water interface were obtained, using Eq. (1), and the results are shown in Fig. 7 (lower panel, symbols). Fitting the Langmuir adsorption isotherm yields the maximum surface concentrations of our surface-modified nanoparticles at the air–water interface $\Gamma_{\max} = 0.783$ (nanofluid no.1), 2.23(3), 4.10 (5), and 2.30 (7) nanoparticles/nm². Evidently, the surface modification of the silica nanoparticles considerably modulates the adsorption of the nanoparticles at the air–water interface.

Also shown in Table 3 are the interfacial tensions of surface-modified silica nanofluids. It is observed that by increasing modifying agent quantity on silica surface, their effect on interfacial tension increases. The impact of nanoparticle concentration on the interfacial tensions of nanofluids no. 1, 3, 5, and 7 is depicted in Fig. 8 (upper panel), demonstrating that at higher concentrations of surface-modified silica nanoparticles, the interfacial tension is modulated much more.

The surface concentrations of our surface-modified silica nanoparticles at the oil–water interface were

Table 3 Surface and interfacial tensions of various 1 wt% surface-modified silica nanofluids

Nanofluid	Surface tension (mN/m)	Interfacial tension (mN/m)
Pure water	71.4 ± .2	28.2 ± .4
Unmodified	68.1 ± .4	27.3 ± .5
1	62.1 ± .9	23.2 ± .3
2	65.4 ± .1	26 ± .3
3	52.6 ± .4	19 ± .4
4	58.1 ± .4	21.2 ± .4
5	44.6 ± .2	14.1 ± .2
6	59.8 ± .5	19.5 ± .4
7	55.3 ± .3	15.2 ± .2

obtained, using Eq. (1), and the results are presented in Fig. 8 (lower panel). Fitting the Langmuir adsorption isotherm yields the maximum surface concentrations of our surface-modified nanoparticles at the oil–water interface $\Gamma_{\max} = 0.774$ (nanofluid no.1), 1.37(3), 1.58 (5), and 1.98 (7) nanoparticles/nm².

It is evident that nanoparticles comprising both agents tend to adsorb at the air–water and oil–water interfaces much more compared to nanoparticles with just one agent. This is due to the environmentally responsive behavior of such nanoparticles that causes nanoparticles to act as surfactants on the interfaces. The part in contact with the aqueous phase expands its hydrophilic groups, and the other part in contact with the oil phase expands its hydrophobic groups so that nanoparticles act like amphiphilic Janus nanoparticles with two distinct hydrophilic and hydrophobic parts. In the oil phase, propyl groups interact with oil components adjacent to the interface and in the aqueous phase PEG groups interact with water molecules strongly. Our measurements indicate 50 % reduction in surface and interfacial tensions in 1 wt% concentration that represents significant improvement in silica nanofluid surface activity.

Contact angle

Captive droplet contact angles of oil–water on the glass slide and carbonate rock section were measured after altering the wettability of the slide and section. As presented in Fig. 9, oil–water contact angles on the slide and section are well above 90°, indicating that their wettability has been changed to strongly oil-wet. After aging glass slides and carbonate rock sections in various nanofluids for 24 h, oil–water contact angles on their surfaces were measured again. As shown in

Fig. 10, surfaces aged in hydrophilic or environmentally responsive silica nanofluids had lower contact angles. Surfaces aged in unmodified or hydrophobic silica nanofluids did not show any clear change in contact angles after 24 h.

Oil–water contact angles on glass slides and carbonate rock sections after 72 h of aging in various nanofluids are displayed in Fig. 11. It is observed that all of the contact angles have been decreased. Surfaces aged in hydrophilic or environmentally responsive silica nanofluids had higher rate of contact angle decrement compared with surfaces aged in the other nanofluids. This fact is highlighted in Fig. 12, representing oil–water captive droplet contact angles on the oil-wetted glass and carbonate rock surfaces versus aging time.

For the case of the carbonate rock section, this observation can be explained by two scenarios. One scenario is the electrostatic interaction between silica surface PEG chains, comprising partially negative ether groups, and charged carbonate rock surface sites such as Ca²⁺ and CO₃²⁻. When carbonate rock is aged for a long time in crude oil, surface Ca²⁺ and CO₃²⁻ sites are considerably covered with charged oil components, and the interaction between silica nanoparticle PEG chains and the sites is not possible. Aging the oil-wetted carbonate rock section in PEGylated silica nanofluids leads to replacing some of oil components attached to the carbonate rock surface with PEGylated silica nanoparticles. Accordingly, positive Ca²⁺ sites on the carbonate rock can interact much more with the ether groups. This results in increased hydrophilicity of the carbonate rock section. The other scenario is the electrostatic interaction between asphaltene components attached on carbonate rock surface and PEG chains. Asphaltene

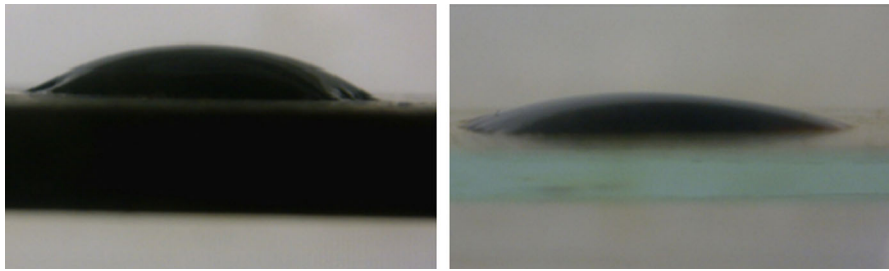


Fig. 9 Contact angles of oil–water on oil-wetted glass slide (*left*) and carbonate rock section (*right*) before aging in nanofluids

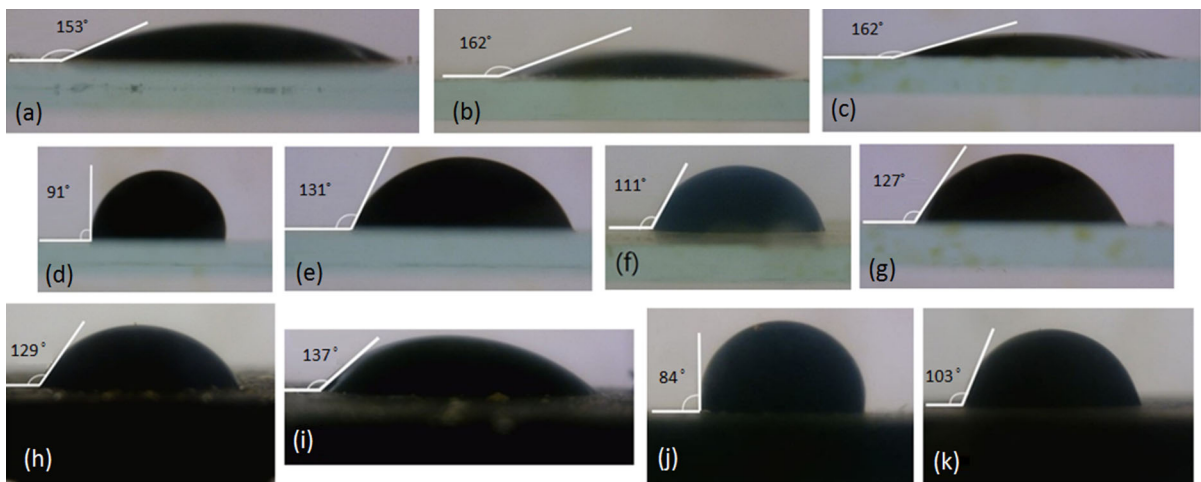


Fig. 10 Captive droplet contact angles of oil–water on oil-wetted glass slides after 24 h of aging in unmodified silica nanofluid (**a**), and nanofluids no. 1 (**b**), 2 (**c**), 3 (**d**), 4 (**e**), 5 (**f**), and 6 (**g**); Captive droplet contact angles of oil–water on oil-

wetted sections of carbonate rock after 24 h of aging in unmodified silica nanofluid (**h**), and nanofluids no. 1 (**i**), 3 (**j**), and 5 (**k**). Concentration of nanoparticles in the nanofluids was 1 wt%. To guide eye, we have flipped the images

molecules have positively charged sites, which can interact electrostatically with partially negative ether groups of PEG chains bonded on the silica nanoparticle surface.

For the case of the glass slide, the observation can be explained by considering possible hydrogen bonds between silica nanoparticle –Si–OH or PEG-chain ether groups and glass –Si–OH surface groups. PEGylating nanoparticles can result in increased adsorption of the nanoparticles on the glass surface due to likely hydrogen bonds from the presence of PEG-chain ether groups. When the PEGylated nanoparticles are adsorbed on the glass surface, the hydrophobicity of the oil-wetted glass slide decreases. Measured contact angles of oil–water on the glass and carbonate rock surfaces that were aged in hydrophilic or environmentally responsive silica nanofluids for

72 h were $\sim 45^\circ$, indicating that PEGylated nanofluids can alter the wettability to water-wet.

Flooding to glass micro-model

We performed our flooding experiments initially on the water-wet micro-model (before wettability alteration). For this purpose, the micro-model was loaded with the crude oil. Processing the images captured from the oil-loaded micro-model revealed that the micro-model porosity was 44 %. Then, double-distilled water was injected into the oil-loaded model, and the oil recovery as a function of the injected water pore volume was determined. Final oil recovery factor, after breakthrough point, was 91 %. This huge recovery factor was expectable because the micro-model was water-wet, and this characteristic is highlighted in

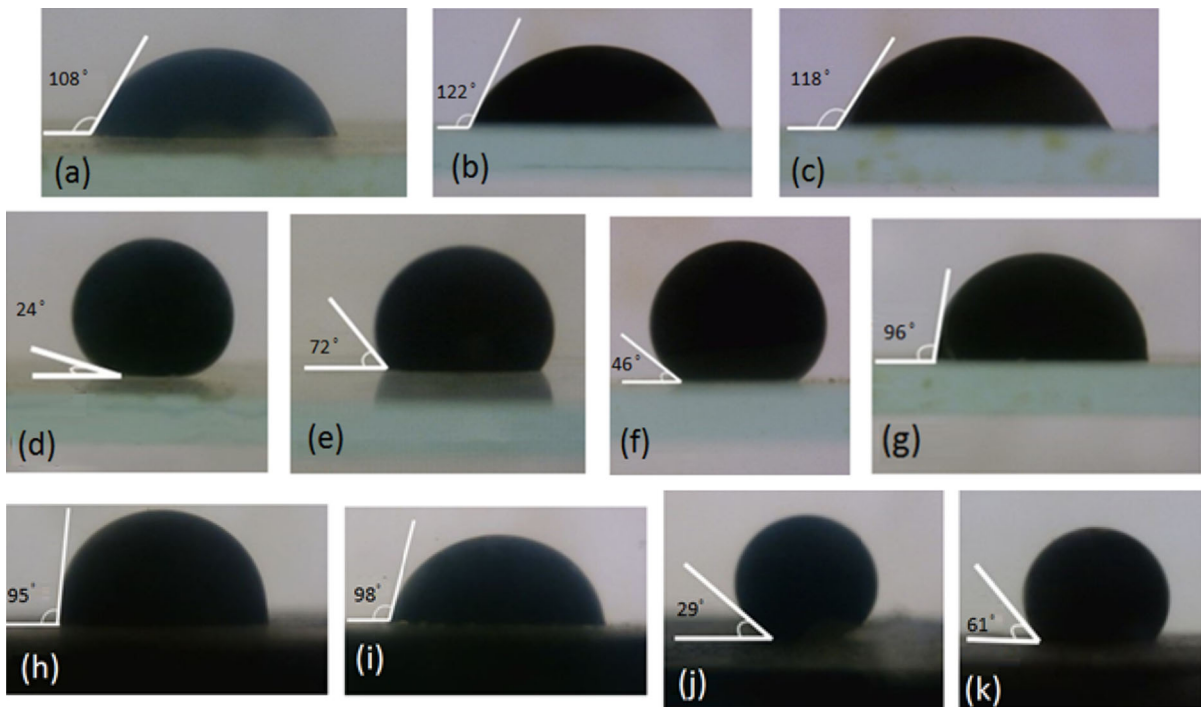


Fig. 11 Captive droplet contact angles of oil–water on oil-wetted glass slides after 72 h of aging in unmodified silica nanofluid (a), and nanofluids no. 1 (b), 2 (c), 3 (d), 4 (e), 5 (f), and 6 (g); (h)–(k) Captive droplet contact angles of oil–water on

oil-wet sections of carbonate rock after 72 h of aging in unmodified silica nanofluid (h), and nanofluids no. 1 (i), 3 (j), and 5 (k). Concentration of nanoparticles in the nanofluids was 1 wt%. To guide eye, we have flipped the images

the microscale pictures captured from the micro-model pores and throats (see Fig. 13a). It is observed that thin oil films have surrounded the micro-model walls, which indicates the micro-model was strongly water-wet.

Then, the water-wet micro-model was made oil-wet, by the procedure explained in “[Flooding to glass micro-model](#)” section, and the resulting oil-wet micro-model was loaded with the crude oil. Afterward, waterflooding experiment was performed. A microscale image of the oil-wet micro-model in the waterflooding experiment is shown in Fig. 13b, which highlights thick oil films around the micro-model pores and throats walls. The presence of the thick oil films reveals that the wettability was altered to oil-wet. Also, the oil recovery factor as a function of the injected water pore volume is shown in Fig. 13h, which illustrates the recovery factor of 39 % after the breakthrough point.

We repeated the flooding experiment with 1 wt% nanofluids. Oil recovery factors as a function of injected nanofluids pore volumes are displayed in

Fig. 13h. It is observed that the oil recovery factor at the breakthrough point for flooding all the nanofluids is more than that of flooding water. Nanofluid no. 1 (with the recovery factor of 47 %) and 5 (with the recovery factor of 59 %) yielded, respectively, the least and the most recovery factors among the nanofluids. The unmodified silica nanofluid performs better, even though slightly, than nanofluid no. 1. Our observations of the recovery factors can be explained by considering the ability of various nanoparticles in modulating oil–water interfacial tension and the oil-wet micro-model wettability. In general, reducing oil–water interfacial tension and altering the micro-model wettability to more water-wet results in higher recovery factors.

Let us examine flooding the unmodified silica nanofluid, which yielded in a considerably higher recovery factor compared with flooding water. Already, it is observed that the interfacial tension of oil–water is not modulated considerably by the unmodified silica nanoparticles (see Fig. 8). Thus, the improvement in the oil recovery can be attributed

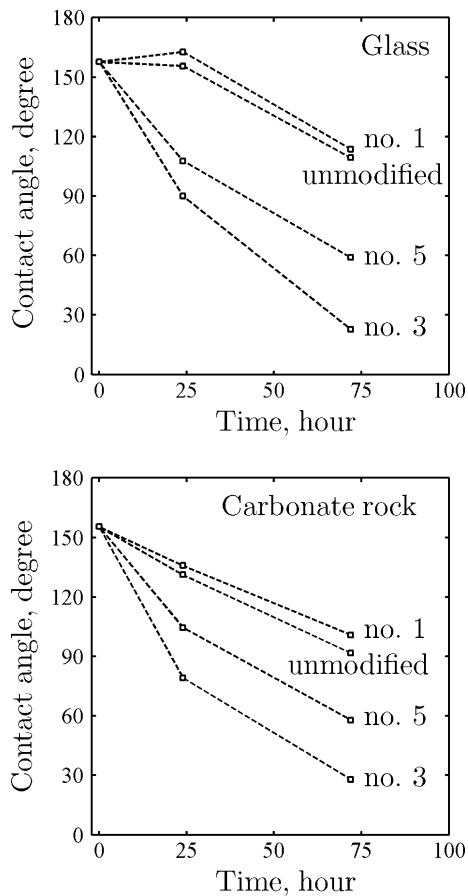


Fig. 12 Captive droplet contact angles of oil–water on oil-wetted glass slides (*left*) and sections of carbonate rock (*right*) after aging in various nanofluids; unmodified silica nanofluid, and nanofluids no. 1, 3, and 5. Concentration of nanoparticles in the nanofluids was 1 wt%

to the oil-wet micro-model wettability alteration. The adsorption of the nanoparticles on the walls of the oil-wet micro-model alters the wettability to water-wet (see Fig. 13c) (Maghzi et al. 2012), and thus, the tendency of the oil to displace by the injected fluid increases.

The other nanofluid flooded to the oil-wet micro-model was nanofluid no. 1, which resulted in lower, even though slightly, recovery factor relative to that of the unmodified silica nanofluid. Recall that nanofluid no. 1 comprises hydrophobic silica nanoparticles, which were able to reduce oil–water interfacial tension more than unmodified silica nanoparticles (see Fig. 8). In addition, it is already observed that the oil was spreading more on oil-wetted glass slides in the presence of the hydrophobic silica nanoparticles

compared with that in the presence of unmodified silica nanoparticles (the observed contact angles were roughly indicator of this phenomenon, see Fig. 12). Ostensibly, the wettability alteration property of the hydrophobic silica nanoparticles is the dominant factor in controlling oil recovery from the oil-wet micro-model. The hydrophobic silica nanoparticles alter the micro-model wettability to water-wet less than the corresponding unmodified silica nanofluid (see Fig. 13c, d).

Injecting nanofluid no. 3 yielded the recovery factor of 54 %. Recall that nanofluid no. 3 comprises PEGylated silica nanoparticles. The improved recovery factor can be due to both the reduction in interfacial tension and wettability alteration. Micro-scale pictures taken from the micro-model in flooding nanofluid no. 3 (Fig. 13e) display thinner oil films around the micro-model pores and throats compared with flooding unmodified or hydrophobic silica nanofluids, indicating PEGylated silica nanofluid performs better in wettability alteration.

Now we focus on the recovery factors obtained from flooding environmentally responsive silica nanofluids. Two environmentally responsive silica nanofluids were used for flooding experiments: nanofluids no. 5 and 6. For the case of nanofluid no. 5, the obtained recovery factor was 59 %, which was even 5 % larger than that of nanofluid no. 3. The improved recovery factor can be attributed to the ability of nanofluid no. 5 in reducing oil–water interfacial tension relative to that of nanofluid no. 3, because environmentally responsive silica nanoparticles tend to adsorb on fluid–fluid interface more than solely hydrophilic silica nanoparticles. However, for the case of flooding nanofluid no. 6, the recovery factor was 51 %, which was even lower than that of silica nanofluid no. 3. The decreased recovery factor, relative to those of nanofluids no. 5 and 3, originates from the smaller quantity of PEG chains coated on the nanofluid no. 6 silica nanoparticles, reducing the wettability alteration ability of the nanoparticles (see Figs. 13e–g).

We note that, in order to interpret more precisely the observed phenomena in our flooding experiments, it is required to account other underlying mechanisms (Mohammed and Babadagli 2015; Zhang et al. 2014) in addition to aforementioned mechanism to develop a more comprehensive understanding of how environmentally responsive mixed polymer-coated

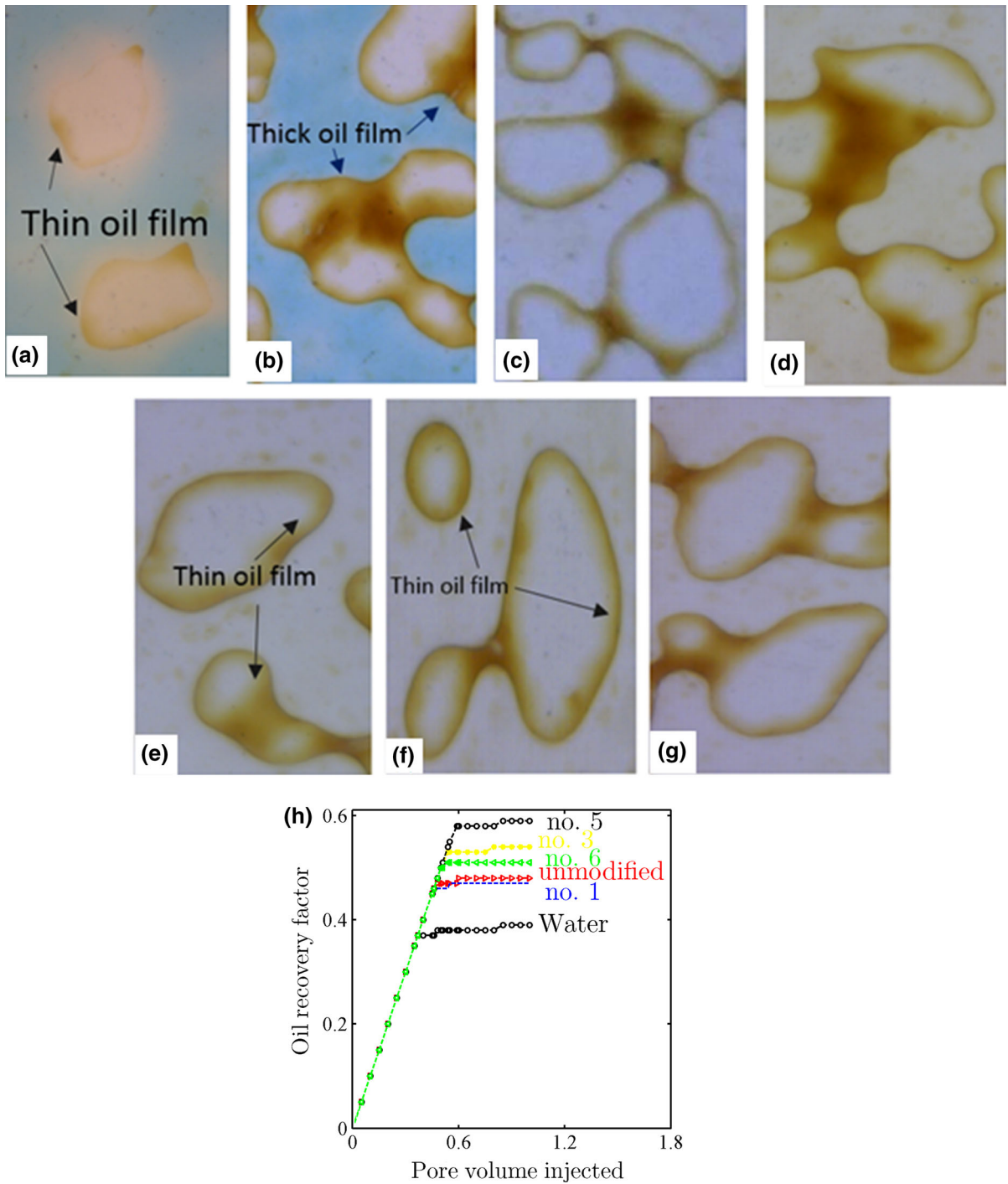


Fig. 13 a–g Typical microscale images from pores and throats of water-wet (a) and oil-wet (b–g) micro-models when various fluids were flooding. Flooded fluids were water (a–b), unmodified silica nanofluid (c), and nanofluids no. 1 (d), 3 (e), 5 (f), and

6 (g); h Oil recovery factor as a function of various injected fluids pore volume: water, unmodified silica nanofluid, and nanofluids no. 1, 3, 5, and 6. Concentration of nanoparticles in the nanofluids was 1 wt%

nanoparticles improve the oil recovery, where this will be undertaken in our future studies both theoretically and experimentally.

In closing, note that the performance of our surface-modified nanoparticles must maintain under the reservoir condition of high temperature with typical range from 40 to 150 °C (see Ranka et al. (2015), and references therein) in order to be employed for enhancement of oil recovery. An influence of increased temperature is on the conformations of surface groups at liquid–liquid and solid–liquid interfaces (Maskey et al. 2016; Schwenke et al. 2014). It is well known that chain molecules swell in good solvent regime and shrink in poor solvents (see Mohammadi et al. (2012), and references therein for a descriptive explanation on poor and good solvents). At low temperatures, or poor solvent conditions, chains shrink due to attractive forces. At high temperatures, or good solvent conditions, chains swell due to repulsive forces. The conformations of the surface groups of our nanoparticles at interfaces, which depend on attractive and repulsive interactions, would be modulated by increased temperatures, and accordingly, the surface activity of the nanoparticles would be different.

Another impact of increased temperature is on the stability of the surface groups. It has been observed that, at elevated temperatures, chemical agents show limited stability and degrade. In this vein, note that we are expecting to have our surface-modified nanoparticles to be stable at temperatures up to, at least, 80 °C as they have been synthesized under long-time refluxes at the temperature of 80 °C (see “[Nanoparticles surface modification](#)” section). However, in line with the recent experimental effort (Ranka et al. 2015), more stable groups can be grafted on the surface of nanoparticles to perform efficiently at elevated temperatures without thermal degradation.

Conclusions

PEG and propyl chains were grafted on silica nanoparticles and results of FT-IR spectra indicated that desired reactions were successfully proceeded. Nanoparticle surface modification impact on the corresponding nanofluid surface activity was monitored by measuring oil-nanofluid interfacial and nanofluid surface tensions. It was observed that increasing modifying agents’ quantities on silica

nanoparticles surface, and also, coating both hydrophilic and hydrophobic agents on silica nanoparticles surface increase the surface activity. Aging various oil-wetted surfaces in unmodified and various surface-modified silica nanofluids and measuring captive droplet contact angles of oil–water on the surfaces demonstrated that surface modification of silica nanoparticles can considerably improve the wettability alteration ability of silica nanoparticles.

Moreover, pore-level investigations of oil-wet micro-models in various flooding experiments with surface-modified silica nanofluids revealed that hydrophilic and environmentally responsive silica nanoparticles can modify considerably the micro-model wettability. Oil recovery factors from the oil-loaded oil-wet micro-model with injecting unmodified and various surface-modified silica nanofluids were monitored. Flooding nanofluids to glass micro-models demonstrated that surface modification of silica nanoparticles, specially, with both hydrophilic and hydrophobic agents improves considerably their performance in increasing oil recovery.

Finally, note that this study is a preliminary study for developing inexpensive environmentally responsive nanomaterials for enhancement of oil recovery to perform efficiently at operational conditions of well reservoirs, including high salinities and temperatures, where this paper provides a basis for further theoretical and experimental investigations.

Acknowledgments A.M. gratefully acknowledges supports from the Sharif University of Technology Research Council and the Iranian National Science Foundation.

References

- Al-Sulaimani H, Al-Wahaibi Y, Al-Bahry S, Elshafie A, Al-Bemani A, Joshi S (2012) Residual-oil recovery through injection of biosurfactant, chemical surfactant, and mixtures of both under reservoir temperatures: induced-wettability and interfacial-tension effects. *SPE Reserv Eval Eng* 15:210–217
- Baran Jr JR, Cabrera OJ (2006) Use of surface-modified nanoparticles for oil recovery. U.S. Patent 7,033,975
- Barnes JR, Groen K, On A, Dubey ST, Reznik C, Buijse MA, Shepherd AG (2012) Controlled hydrophobe branching to match surfactant to crude composition for chemical EOR. *SPE Improved Oil Recovery Symposium*
- Bauer RG, Klemmensen DF (1982) A new polymer for enhanced oil recovery. *SPE Enhanced Oil Recovery Symposium*

- Bera A, Mandal A, Guha B (2013) Synergistic effect of surfactant and salt mixture on interfacial tension reduction between crude oil and water in enhanced oil recovery. *J Chem Eng Data* 59:89–96
- Binks BP, Whitby CP (2004) Silica particle-stabilized emulsions of silicone oil and water: aspects of emulsification. *Langmuir* 20:1130–1137
- Chaudhuri RG, Paria S (2014) Effect of electrolytes on wettability of glass surface using anionic and cationic surfactant solutions. *J Colloid Interface Sci* 413:24–30
- Clark HP, Ascanio FA, Van Kruijsdijk CP, Chavarria JL, Zatkan MJ, Williams W, Yahyai AH, Shaw JD, Bedry M (2010) Method to improve thermal EOR performance using intelligent well technology: Orion SAGD field trial. Canadian Unconventional Resources and International Petroleum Conference
- Coates J (2000) Interpretation of infrared spectra, a practical approach. In: Meyers RA (ed) *Encyclopedia of analytical chemistry*. Wiley, Chichester, pp 10815–10837
- Dietrich F, Brown F, Zhou Z, Maure M (1996) Microbial EOR technology advancement: case studies of successful projects. SPE Annual Technical Conference and Exhibition
- Fan H, Striolo A (2012) Nanoparticle effects on the water-oil interfacial tension. *Phys Rev E* 86:051610
- Green DW, Willhite GP (1998) Enhanced oil recovery. Henry L. Doherty Memorial Fund of AIME. Society of Petroleum Engineers, Richardson
- Hirasaki GJ, Miller CA, Puerto M (2008) Recent advances in surfactant EOR. SPE Annual Technical Conference and Exhibition
- Hotze EM, Phenrat T, Lowry GV (2010) Nanoparticle aggregation: challenges to understanding transport and reactivity in the environment. *J Environ Qual* 39:1909–1924
- Hunter RJ (2001) *Foundations of colloid science*. Oxford University Press, Oxford
- Jamaloeei BY, Kharrat R (2010) Analysis of microscopic displacement mechanisms of dilute surfactant flooding in oil-wet and water-wet porous media. *Transp Porous Med* 81:1–19
- Jassby D (2011) Impact of particle aggregation on nanoparticle reactivity. Dissertation, Duke University
- Jiang J, Oberdörster G, Biswas P (2009) Characterization of size, surface charge, and agglomeration state of nanoparticle dispersions for toxicological studies. *J Nanopart Res* 11:77–89
- Johannessen AM, Spildo K (2013) Enhanced oil recovery (EOR) by combining surfactant with low salinity injection. *Energy Fuel* 27:5738–5749
- Kamal M, Sultan A, Al-Mubaiyedh U, Hussein I, Pabon M (2014) Evaluation of rheological and thermal properties of a new fluorocarbon surfactant–polymer system for EOR applications in high-temperature and high-salinity oil reservoirs. *J Surfactants Deterg* 17:985–993
- Kang, X, Jian Z, Fujie S, Fengjiu Z, Guozhi F, JunRu Y, Xiansong Z, Wentao X (2011) A review of polymer EOR on offshore heavy oil field in Bohai Bay, China. SPE Enhanced Oil Recovery Conference
- Karimi A, Fakhroueian Z, Bahramian A, Pour Khiabani N, Darabad JB, Azin R, Arya S (2012) Wettability alteration in carbonates using zirconium oxide nanofluids: EOR implications. *Energy Fuel* 26:1028–1036
- Kim I, Worthen AJ, Johnston KP, DiCarlo DA, Huh C (2016) Size-dependent properties of silica nanoparticles for Pickering stabilization of emulsions and foams. *J Nanopart Res* 18:1–12
- Klint A (2011) Amphiphilic surface modification of colloidal silica sols. Dissertation, Chalmers University of Technology
- Le NYT, Pham DK, Le KH, Nguyen PT (2011) Design and screening of synergistic blends of SiO₂ nanoparticles and surfactants for enhanced oil recovery in high-temperature reservoirs. *Adv Nat Sci: Nanosci Nanotechnol* 2:035013
- Levitt D, Pope GA (2008) Selection and screening of polymers for enhanced-oil recovery. SPE Symposium on Improved Oil Recovery
- Lim S, Horiuchi H, Nikolov AD, Wasan D (2015) Nanofluids alter the surface wettability of solids. *Langmuir* 31:5827–5835
- Maghzi A, Mohammadi S, Ghazanfari MH, Kharrat R, Masihi M (2012) Monitoring wettability alteration by silica nanoparticles during water flooding to heavy oils in five-spot systems: a pore-level investigation. *Exp Therm Fluid Sci* 40:168–176
- Maskey S, Lane JMD, Perahia D, Grest GS (2016) Structure of rigid polymers confined to nanoparticles: molecular dynamics simulations insight. *Langmuir* 32:2102–2109
- Metin CO, Baran JR Jr, Nguyen QP (2012) Adsorption of surface functionalized silica nanoparticles onto mineral surfaces and decane/water interface. *J Nanopart Res* 14:1–16
- Mohammadi A, Saadatabadi AR, Khanpour M (2012) Second virial coefficients of Exp-6 chains: a Monte Carlo simulation. *Chem Phys* 397:26–33
- Mohammed M, Babadagli T (2015) Wettability alteration: a comprehensive review of materials/methods and testing the selected ones on heavy-oil containing oil-wet systems. *Adv Colloid Interface Sci* 220:54–77
- Monfared AD, Ghazanfari M, Jamialahmadi M, Helalizadeh A (2015) Adsorption of silica nanoparticles onto calcite: equilibrium, kinetic, thermodynamic and DLVO analysis. *Chem Eng J* 281:334–344
- Morrow NR (1990) Wettability and its effect on oil recovery. *J Pet Technol* 42:1,476–471,484
- Puerto M, Hirasaki GJ, Miller CA, Barnes JR (2012) Surfactant systems for EOR in high-temperature, high-salinity environments. *SPE J* 17:11–19
- Ramirez WF (1987) Application of optimal control theory to enhanced oil recovery, vol 21. Elsevier, Amsterdam
- Ranka M, Brown P, Hatton TA (2015) Responsive stabilization of nanoparticles for extreme salinity and high-temperature reservoir applications. *ACS Appl Mater Interfaces* 7:19651–19658
- Rodriguez Pin E, Roberts M, Yu H, Huh C, Bryant SL (2009) Enhanced migration of surface-treated nanoparticles in sedimentary rocks. SPE Annual Technical Conference and Exhibition
- Rosen MJ, Wang H, Shen P, Zhu Y (2005) Ultralow interfacial tension for enhanced oil recovery at very low surfactant concentrations. *Langmuir* 21:3749–3756
- Rostami M, Mohseni M, Ranjbar Z (2011) Investigating the effect of pH on the surface chemistry of an amino silane treated nano silica. *Pigment Resin Technol* 40:363–373
- Roustaei A, Bagherzadeh H (2015) Experimental investigation of SiO₂ nanoparticles on enhanced oil recovery of carbonate reservoirs. *J Pet Explor Prod Technol* 5:27–33

- Schwenke K, Isa L, Cheung DL, Del Gado E (2014) Conformations and effective interactions of polymer-coated nanoparticles at liquid interfaces. *Langmuir* 30:12578–12586
- Sen R (2008) Biotechnology in petroleum recovery: the microbial EOR. *Prog Energ Combust* 34:714–724
- Shaker Shiran B, Skauge A (2013) Enhanced oil recovery (EOR) by combined low salinity water/polymer flooding. *Energy Fuel* 27:1223–1235
- ShamsiJazeyi H, Miller CA, Wong MS, Tour JM, Verduzco R (2014) Polymer-coated nanoparticles for enhanced oil recovery. *J Appl Polym Sci* 131:40576–40589
- Somasundaran P, Zhang L (2006) Adsorption of surfactants on minerals for wettability control in improved oil recovery processes. *J Pet Sci Eng* 52:198–212
- Suleimanov B, Ismailov F, Veliyev E (2011) Nanofluid for enhanced oil recovery. *J Pet Sci Eng* 78:431–437
- Suttioponparmit K, Jiang J, Sahu M, Suvachittanont S, Charinpanitkul T, Biswas P (2011) Role of surface area, primary particle size, and crystal phase on titanium dioxide nanoparticle dispersion properties. *Nanoscale Res Lett* 6:27
- Thomas S (2008) Enhanced oil recovery-an overview. *Oil Gas Sci Technol-Rev l'IFP* 63:9–19
- Wang KL, Liang SC, Wang CC (2010) Research of improving water injection effect by using active SiO₂ nano-powder in the low-permeability oilfield. *Adv Mat Res* 92:207–212
- Wang Y, Fan D, He J, Yang Y (2011) Silica nanoparticle covered with mixed polymer brushes as Janus particles at water/oil interface. *Colloid Polym Sci* 289:1885–1894
- Watkins C (2009) Chemically enhanced oil recovery stages a comeback. *Inform* 20:682–685
- Zargartalebi M, Barati N, Kharrat R (2014) Influences of hydrophilic and hydrophobic silica nanoparticles on anionic surfactant properties: interfacial and adsorption behaviors. *J Pet Sci Eng* 119:36–43
- Zhang H, Nikolov A, Wasan D (2014) Enhanced oil recovery (EOR) using nanoparticle dispersions: underlying mechanism and imbibition experiments. *Energy Fuel* 28:3002–3009
- Zhao B, Zhu L (2009) Mixed polymer brush-grafted particles: a new class of environmentally responsive nanostructured materials. *Macromolecules* 42:9369–9383
- Zhao X, Blunt MJ, Yao J (2010) Pore-scale modeling: effects of wettability on waterflood oil recovery. *J Pet Sci Eng* 71:169–178